ACS Catalysis

pubs.acs.org/acscatalysis

Research Article

Photoinduced Iron-Catalyzed *ipso*-Nitration of Aryl Halides via Single-Electron Transfer

Cunluo Wu,[‖] Qilong Bian,[‖] Tao Ding, Mingming Tang, Wenkai Zhang, Yuanqing Xu, Baoying Liu, Hao Xu,* Hai-Bei Li,* and Hua Fu*

Cite This: *ACS Catal.* 2021, 11, 9561−9568

Read Online

ACCESS | Metrics & More | Article Recommendations | Supporting Information

ABSTRACT: A photoinduced iron-catalyzed *ipso*-nitration of aryl halides with KNO_2 has been developed, in which aryl iodides, bromides, and some of aryl chlorides are feasible. The mechanism investigations show that the *in situ* formed iron complex by $FeSO_4$, KNO_2, and 1,10-phenanthroline acts as the light-harvesting photocatalyst with a longer lifetime of the excited state, and the reaction undergoes a photoinduced single-electron transfer (SET) process. This work represents an example for the photoinduced iron-catalyzed Ullmann-type couplings.

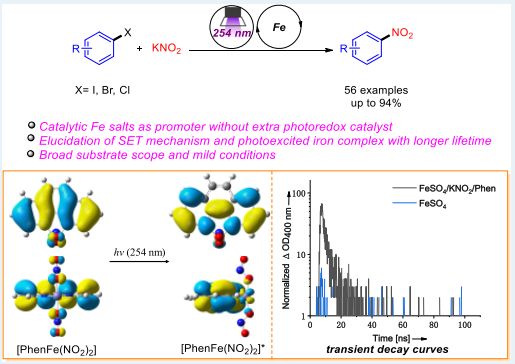

KEYWORDS: *photoinduced, iron catalyzed, ipso-nitration, aryl halides, SET mechanism*

INTRODUCTION

Aromatic nitro compounds and their derivatives are prevalent synthons in pharmaceuticals, pesticides, functional materials, and diverse intermediates in organic synthesis.[1] Most studies on the synthesis of aromatic nitro compounds have focused on electrophilic nitration of arenes, leading to low region selectivity and overnitration.[2] To resolve this issue, *ipso*-nitration of aryl bromides and iodides was performed to produce these compounds via copper-catalyzed Ullmann-type couplings (Scheme 1A).[3] In recent years, the *ipso*-nitration of aryl chlorides has been achieved under palladium-catalyzed conditions by Buchwald and Fors (Scheme 1A).[4] Compared with expensive transition-metal catalysis, iron-catalyzed coupling reactions are obviously cost-effective. However, iron-catalyzed *ipso*-nitration of aryl halides has not been reported thus far.

In the aforementioned copper- or palladium-catalyzed *ipso*-nitration of aryl halides, the mechanisms were proposed via an oxidative addition/reductive elimination process (two-electron transfer).[3,4] Indeed, iron complexes can engage in two-electron transfer procedures.[5] However, single-electron transfer (SET) is competitive and preferred in some situations.[6] Furthermore, the formal valence states of iron range from −II to +VI, and the limited stability of (organo)iron complexes with low or high oxidation states may lead to complex reactivity profiles.[7] Therefore, the iron-catalyzed *ipso*-nitration of aryl halides could not be taken for granted, and mechanistic investigations into iron catalysis are complicated.

In recent years, photopromoted Ullmann- and Buchwald-type coupling reactions of aryl halides with various nucleophile agents (such as heteroaromatic nitrogen nucleophiles, amines, thiols, and phenols) have received significant attention (Scheme 2).[8] Furthermore, copper and nickel catalysts are always employed as photoredox catalysts in the reactions. However, until now, using iron complexes as photoredox catalysts for organic transformation has been rare.[9] Very recently, photopromoted iron-catalyzed Kumada coupling of aryl halides with aliphatic Grignard reagents has been developed by Noël and Alcázar (Scheme 3)[9a] in the presence of the Grignard reagent as a strong electron donor (E_{ox} = 0.4 V vs Mg RE.),[10] and a two-electron transfer mechanism is proposed. However, without strong electron donors as substrates (for example, potassium nitrite as the substrate in this work; E_{ox} = 2.031 V vs saturated calomel electrode (SCE), Figure S1), it can be questioned whether the photopromoted coupling of aryl halides with nitrites could be realized and which mechanism (SET vs two-electron transfer) could be preferred? Furthermore, the application of iron as an earth-abundant metal in photocatalysis is highly desirable, but it is

Received: May 20, 2021
Revised: June 8, 2021
Published: July 16, 2021

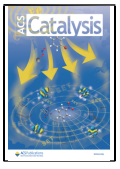

https://doi.org/10.1021/acscatal.1c02272
ACS Catal. 2021, 11, 9561−9568

Scheme 1. *ipso*-Nitration of Aryl Halides

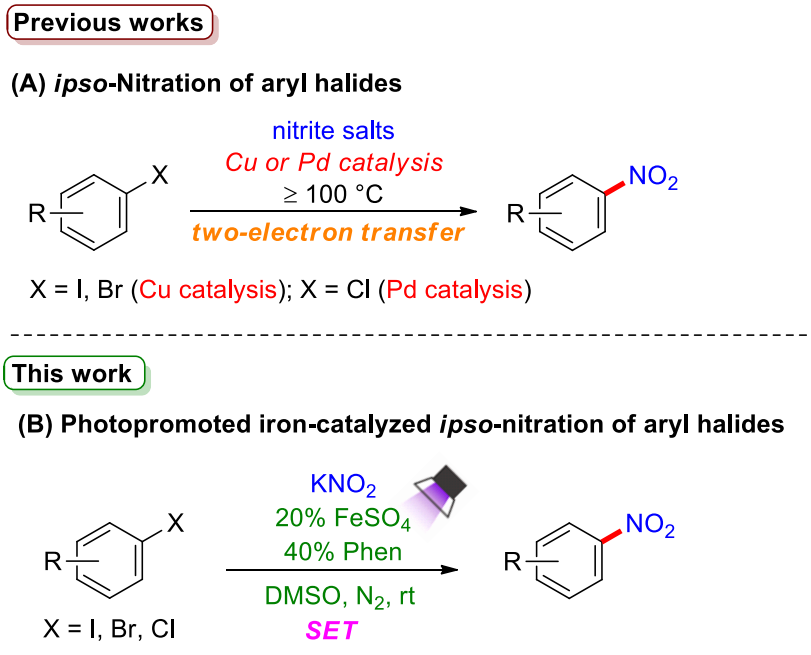

Scheme 2. Photopromoted Ullmann- and Buchwald-Type Couplings

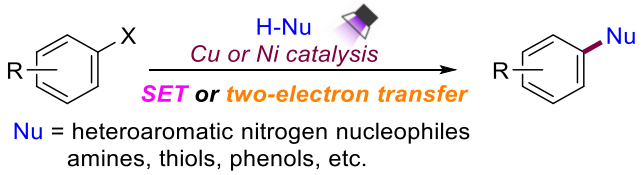

Scheme 3. Photoinduced Iron-Catalyzed Kumada Coupling in Flow

usually hindered by a particularly short lifetime due to low-lying iron-centered electronic states.[11] Whether do the photoexcitable iron complex in this reaction has enough lifetime of excited state to promote this transformation? In this research, the photoinduced iron-catalyzed *ipso*-nitration of aryl halides is achieved (Scheme 1B), employing KNO_2 as the nitration reagent. This method tolerates not only aryl iodides/bromides but also some aryl chlorides. Moreover, a photoexcited iron complex of $FeSO_4$ with KNO_2 and 1,10-phenanthroline (Phen) is proposed as a key intermediate with a longer lifetime. Additionally, it is found that a SET process from this iron(II) complex to aryl halide is preferred under photopromoted conditions. Following this strategy, various aromatic nitro compounds including three pharmaceutical molecules are smoothly prepared from aryl halides and KNO_2.

RESULTS AND DISCUSSION

At the initial stage of the investigations, we treated model substrates of 1-iodo-4-methoxybenzene (**1y**) and KNO_2 with Phen (40 mol %) and $FeSO_4$ (20 mol %) under irradiation at 254 nm and a nitrogen atmosphere for 48 h at room temperature (~25 °C). To maintain a constant temperature of the quartz reaction tube, a thermostat with a cooling system was employed (Figure S2). Surprisingly, 1-methoxy-4-nitrobenzene (**2y**) was obtained in 73% yield (Table 1, entry 1).

Table 1. Optimization of Reaction Conditions[a]

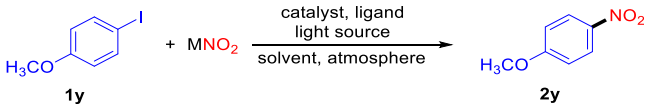

entry	energy source	catalyst	ligand	solvent	yield (%)[b]
1	254 nm	$FeSO_4$	Phen	DMSO	73
2	365 nm	$FeSO_4$	Phen	DMSO	trace
3[c]	Xe lamp	$FeSO_4$	Phen	DMSO	trace
4	blue LED	$FeSO_4$	Phen	DMSO	0
5	green LED	$FeSO_4$	Phen	DMSO	0
6	dark	$FeSO_4$	Phen	DMSO	0
7	130 °C	$FeSO_4$	Phen	DMSO	trace
8	254 nm	FeS	Phen	DMSO	51
9	254 nm	$FeCl_3$	Phen	DMSO	31
10	254 nm	Ferrocene	Phen	DMSO	49
11	254 nm	Fe_3O_4	Phen	DMSO	trace
12	254 nm		Phen	DMSO	9
13	254 nm	$FeSO_4$	2,2′-bipyridine	DMSO	68
14	254 nm	$FeSO_4$	Phen	DMF	trace
15[d]	254 nm	$FeSO_4$	Phen	DMSO	57
16[e]	254 nm	$FeSO_4$	Phen	DMSO	37
17[f]	254 nm	$FeSO_4$	Phen	DMSO	20
18[g]	254 nm	$FeSO_4$	Phen	DMSO	27

[a]Reaction conditions: **1y** (0.3 mmol), nitrite salt (0.9 mmol), catalyst (0.06 mmol), ligand (0.12 mmol), anhydrous solvent (1.0 mL), stirred for 48 h at room temperature under N_2 and irradiation from light source. [b]Yield of the isolated compound. [c]Xe lamp = xenon lamp (400−700 nm). [d]$NaNO_2$ as a nitration reagent. [e]*n*-Bu_4NNO_2 as a nitration reagent. [f]Under an oxygen atmosphere. [g]In air.

https://doi.org/10.1021/acscatal.1c02272
ACS Catal. 2021, 11, 9561−9568

Scheme 4. Scope of Halides[abc]

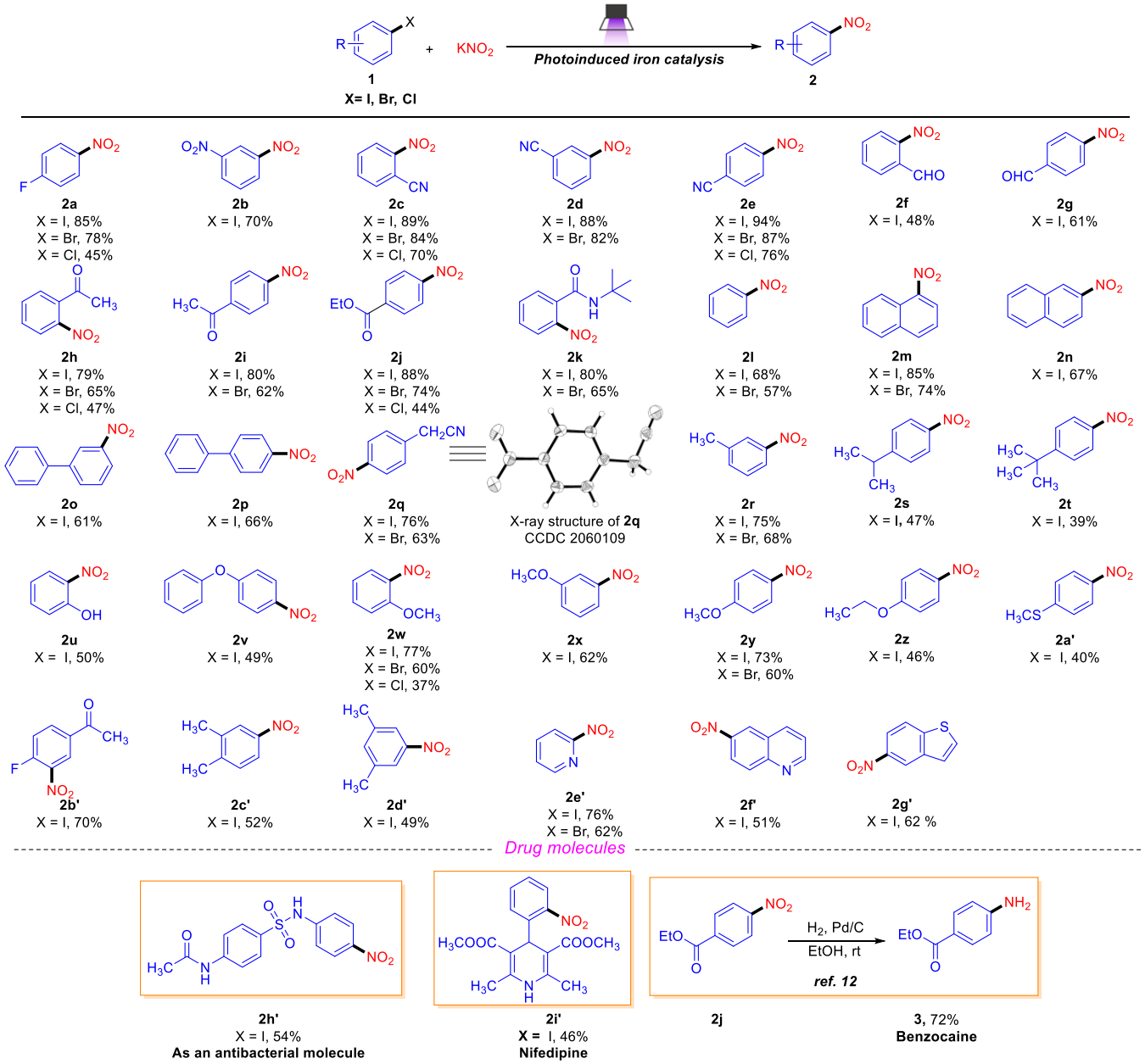

[a]Conditions for aryl iodines: aryl iodine (0.3 mmol), KNO_2 (0.9 mmol), $FeSO_4$ (0.06 mmol), Phen (0.12 mmol), anhydrous DMSO (1.0 mL), stirred for 48 h at room temperature under N_2 and irradiation at 254 nm. [b]Conditions for aryl bromides or chlorides: aryl bromide or chloride (0.3 mmol), KNO_2 (0.9 mmol), $FeSO_4$ (0.06 mmol), Phen (0.12 mmol), KI (0.06 mmol), anhydrous DMSO (1.0 mL), stirred for 48 h at room temperature under N_2 and irradiation at 254 nm. [c]Yield of the isolated compound.

According to the UV−vis absorption spectra of the substrates, Phen, $FeSO_4$, and their mixtures (Figure S3), several irradiation sources were screened, and the model reaction obtained higher yield by irradiating UV light at 254 nm (compare entry 1 with entries 2−5 in Table 1). No reaction occurred under dark conditions (entry 6). Furthermore, the reaction did not work when the reaction system was heated (130 °C) for 48 h without irradiation of light (entry 7). Some photosensitizers were also tested to promote the model reaction under visible light irradiation, and only low yields of **2y** were obtained (Table S1). Moreover, the influence of iron catalysts, ligands, solvents, and reaction atmospheres was also investigated. $FeSO_4$ showed higher efficiency than other iron-based catalysts examined (see entry 1 and entries 8−11), only a small amount of **2y** was isolated without the addition of iron catalysts (entry 12). Among the screened ligands (entry 1 vs entry 13 vs Table S2), Phen was the most efficient for this transformation. After evaluating various solvents, we found that dimethyl sulfoxide (DMSO) was the best choice (entry 1 vs entry 14 vs Table S3), probably due to the good solubility for the substrates. Additionally, two other nitrite salts were also tested (entries 15−16), and KNO_2 was more efficient in generating the desired product **2y** because of better solubility and stability. Meanwhile, several unidentified products were formed when *n*-Bu_4NNO_2 was used as the nitration reagent (entry 16). Besides, switching the atmosphere from N_2 to O_2

https://doi.org/10.1021/acscatal.1c02272
ACS Catal. 2021, 11, 9561−9568

or open-air led to a pronounced yield decrease (entries 17–18), showing that the existence of O_2 was unfavorable for this reaction. In two comparison experiments, the iron-catalyzed *ipso*-nitration was not achieved efficiently under previous thermal conditions in Buchwald's and Kantam's works,[3b,4a] replacing the catalysts of $Pd_2(dba)_3$ and $Cu(OSO_2CF_3)_2$ with $FeSO_4$ (Table S4).

With the as-optimized reaction conditions (Table 1, entry 1), the scope of *ipso*-nitration of aryl iodines was investigated. As exemplified in Scheme 4, all of the investigated aryl iodines provided the corresponding nitration products in moderate to good yields (39–94%). Electron-withdrawing groups (fluoro, nitro, cyano, formyl, acetyl, ester, and amido groups) and electron-donating groups (alkyl, hydroxyl, phenoxy, and methoxy groups) at *ortho*-, *meta*-, and *para*-positions of aryl iodines were well tolerated. Furthermore, the substrates with electron-withdrawing substituents on the phenyl group afforded slightly higher yields than those with electron-donating substituents (**2a**–**k** vs **2r**–**y**). Besides, heteroaromatic iodides could also be transformed into the corresponding nitration products **2e′**–**2g′**. Finally, three drug molecules (**2h′**, **2i′**, and **3**) were also obtained by using our method.[12]

To further explore the scope of substrates, aryl bromides and chlorides were employed as the substrates to perform the *ipso*-nitration with KNO_2 (Scheme 4). Moderate to good yields of nitration products were obtained in the presence of catalytic amount of KI (Table S5). Moreover, the aryl halides with electron-withdrawing substituents on the phenyl group showed higher reactivity (**2a**, **2c**, **2e**, **2h**, and **2j**). Finally, a gram-scale experiment was carried out under similar light-assisted and iron(II)-catalyzed conditions, and the product (**2e**) was obtained in 85% yield (Scheme 5).

Scheme 5. A Gram-Scale Study

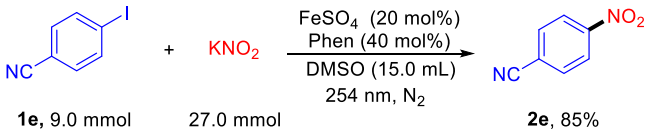

To gain insight into the mechanism of the iron-catalyzed *ipso*-nitration, a radical trapping experiment with **1h** as the substrate and 2,2,6,6-tetramethylpiperidinyloxyl (TEMPO) as the radical trapper was conducted under the standard conditions (Scheme 6A). Only a trace amount of product **2h** was obtained, and the radical adduct with TEMPO was detected by electrospray ionization-high-resolution mass spectrometry (ESI-HRMS) (Figure S4). Moreover, the radical experiment using 1,1-diphenylethylene as the radical scavenger was also performed; the transformation was also suppressed sufficiently (Scheme 6B; Figure S5). These results indicated that a radical intermediate was involved. Furthermore, a competition experiment between 1-bromonaphthalene and 4-chlorobenzonitrile was carried out, and the ratio of products was 4.5:1 under our conditions for the photoinduced *ipso*-nitration of aryl halides (Scheme 7; see Section 9 in the Supporting Information for details). The results implied that a SET mechanism was favored,[8d,a] as opposed to classical oxidative addition in iron-catalyzed Ullmann couplings.[13] The apparent quantum yield of the model reaction of **1i** was measured to be 11.4% (see Section 10 in the Supporting Information for details), implying that continuous irradiation was essential for this transformation, which was consistent with the result of the ON/OFF experiment (Figure 1a, see Section 11 in the Supporting Information for details). In this way, a radical-chain process was unlikely to be a predominant pathway.

Scheme 7. Competition Experiment

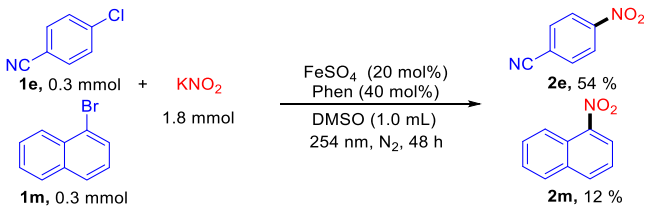

The lifetime of the excited singlet state ($FeSO_4/KNO_2$/Phen) was determined by time-resolved fluorescence spectroscopy (2.95 ns). Without a ligand of Phen, the single iron salt shown in Figure 1b had no fluorescence, and no lifetime decay was detected. Iron complexes are well known for their very short (picosecond) excited-state lifetime.[11] However, under the combined effect of the nitro group and Phen, the iron

Scheme 6. Radical Trapping Experiments

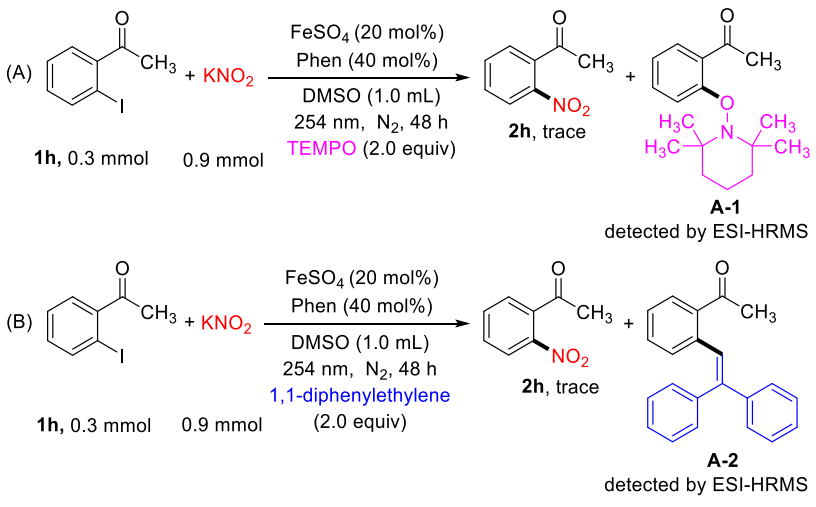

https://doi.org/10.1021/acscatal.1c02272
ACS Catal. 2021, 11, 9561–9568

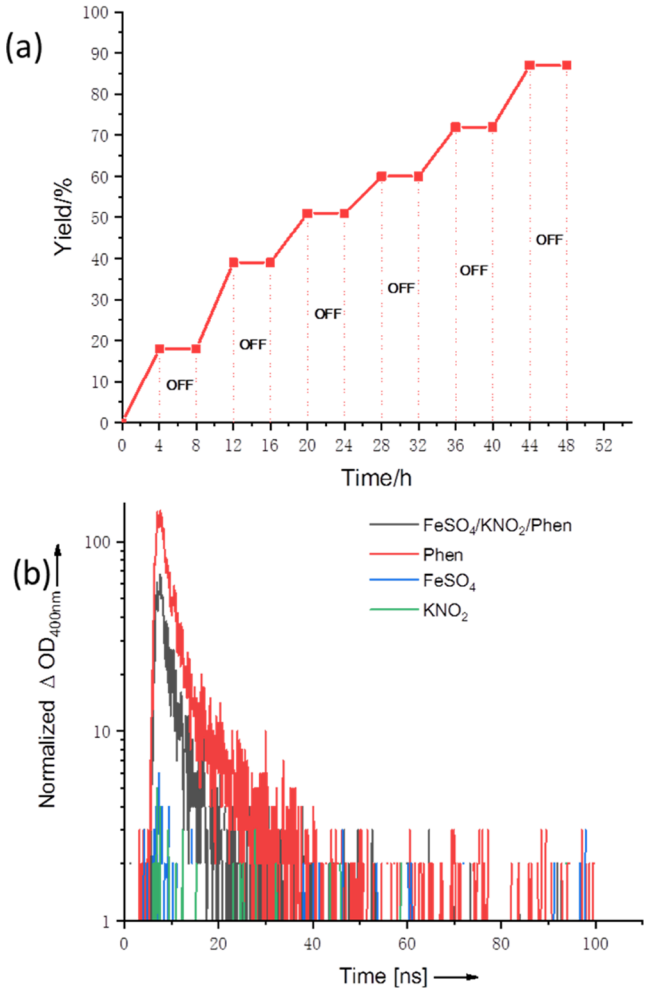

Figure 1. (a) ON/OFF experiment. (b) Decay of each component at 400 nm monitored by laser flash photolysis.

complex's excited-state lifetime was obviously prolonged to promote the reaction. In addition, the time-resolved fluorescence spectra of $FeSO_4/KNO_2$ and $FeSO_4$/Phen were also tested (Figure S7), and the lifetime extension of iron complex's excited-state was mainly due to the interaction of the Phen ligand with $FeSO_4$.

To further explore the mechanism, hybrid functional B3LYP was applied to optimize the geometries of PhenFe(II)$(NO_2)_2$ (**A**) and PhenFe(III)$(NO_2)_2$I (**B**) (see Section 13 in the Supporting Information for details). Both geometries were confirmed to be at the local minimum on the potential surface by vibrational analysis. The time-dependent density functional theory (TD-DFT) method was used to calculate the excited state of **A**. The solvent effect (DMSO) was considered with the polarizable continuum model. As shown in Figure 2, the electron of PhenFe(II)$(NO_2)_2$ (**A**) jumped from the ground state to its excited state **A*** under irradiation of UV light, and the calculated energy level difference (261 nm; **A** to **A***) matched with the experimental data (254 nm in Table 1). Furthermore, the electron's jump in Figure 2a accounted for a contribution of 64 and 30% in Figure 2b. In this case, the electron was transferred from the π-bonding orbital of the Phen ligand to the π^*-antibonding orbital and the 3d orbital of Fe. Moreover, this electron transfer made the excited state **A*** more stable, and the fluorescence lifetime of **A*** (2.95 ns in Figure 1b) was prolonged in comparison with a single $FeSO_4$.

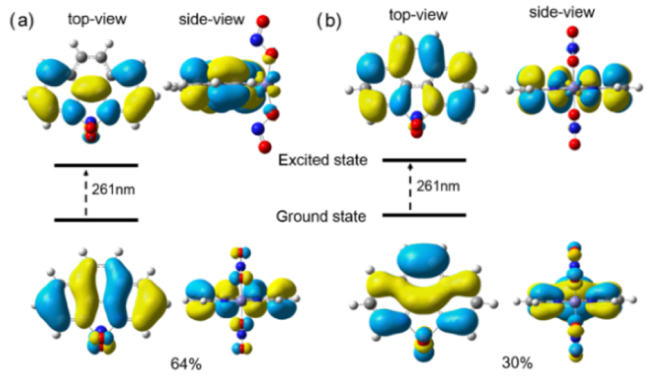

Figure 2. Calculated electronic transition orbitals of PhenFe(II)-$(NO_2)_2$ from the ground state to the excited state using natural transition orbitals (NTO) analysis. (a) Dominant NTO pair. (b) Secondary NTO pair. Both cases are of electron transition from the π-bonding orbital to the π^*-antibonding orbital of the phenanthroline ligand.

Additionally, aryl halides obtained electrons from **A*** to form the iron complex **B** and aryl radicals; the optimal structure of **B** is described in Figure 3 by DFT calculation, and no other structure with higher valence states, such as PhenFe(IV)-$(NO_2)_2I_2$, was formed based on the calculations.

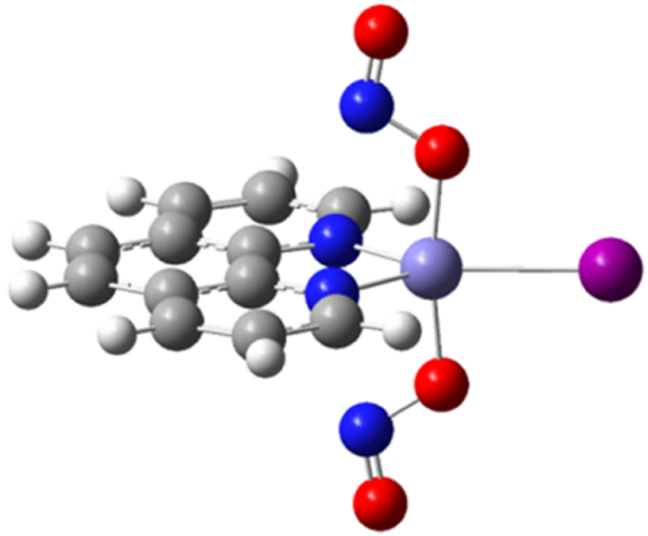

Figure 3. Optimized structure of **B** by DFT calculation.

The redox potential of the 1:2:1 mixture of $FeSO_4/KNO_2$/Phen was measured and calculated to be E_{red} (B/A*) = −3.59 V vs SCE (see Section 14 in the Supporting Information for details), which was lower than E_{red} (**1l**) = −2.24 V vs SCE.[14] These results showed that the complex of $FeSO_4/KNO_2$/Phen could provide a single electron to the iodobenzene **1l** under photopromoted conditions. Furthermore, the fluorescence at 455 nm (emission maximum) emitted by $FeSO_4/KNO_2$/Phen was monitored when the reaction was excited by UV light (Figure S9), and the fluorescence intensity gradually decreased with the titration of **1i** (Figure 4a,b, see Section 15 in the Supporting Information for details). This implied a single-electron transfer between **1i** and the complex of $FeSO_4/KNO_2$/Phen. However, both the iron complex (electron donor) and substrate **1i** (electron acceptor; Figure S12) had close emission maximums (455 vs 469 nm) as well as broad

https://doi.org/10.1021/acscatal.1c02272
ACS Catal. 2021, 11, 9561−9568

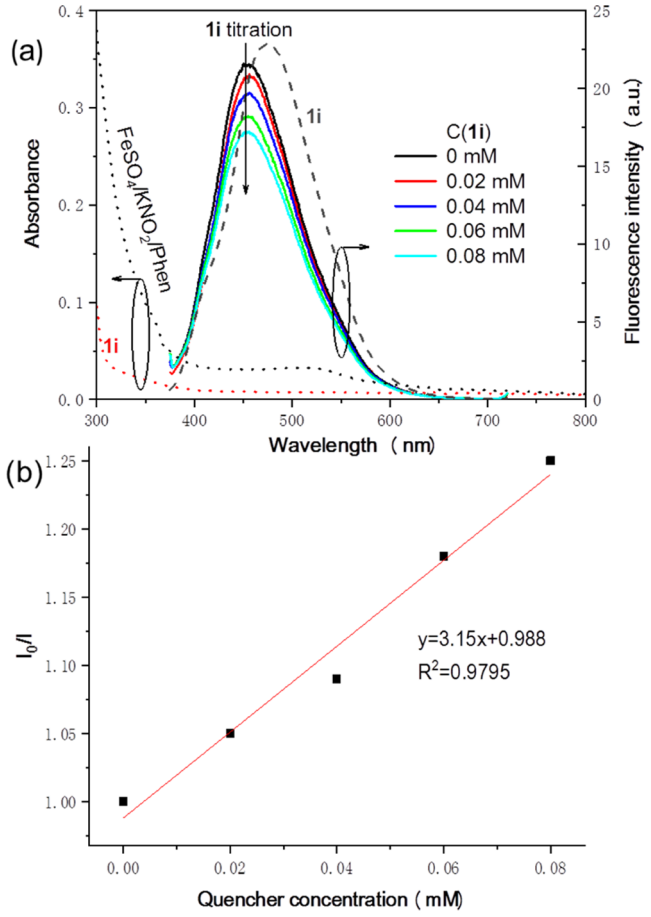

Figure 4. (a) Fluorescence quenching of $FeSO_4/KNO_2$/Phen with different concentrations of **1i** as a quencher. (b) Stern−Volmer plot of $FeSO_4/KNO_2$/Phen at different concentrations of **1i**.

full widths at half-maximum (102 vs 103 nm), showing a significant spectral overlapping in their emission. Due to a concomitant radiative energy transfer between the excited iron complex and substrate **1i**, the spectral enhancement of **1i** partly weakened the fluorescence quenching effect of $FeSO_4/KNO_2$/Phen.

Based on the control experiments mentioned above, TD-DFT calculations, and previous reports,[9,15] a photoinduced iron-catalyzed SET mechanism was proposed (Scheme 8). Initially, iron(II) sulfate could form the iron(II) nitrate complex **A** in the presence of KNO_2 and Phen. Concurrently, the complex **A** reaches its excited state **A*** under the photoinduced conditions. Next, a single-electron transfer from **A*** to aryl iodide takes place, generating the iron(III) complex **B** and an aryl radical. Then, the aryl radical reacts with **B** to produce the target compound **2** and the iron(II) complex **C**. Finally, an anionic exchange of an iodide ion and a nitrite ion occurs and closes the photoinduced catalytic cycle.

CONCLUSIONS

We have developed a photoinduced iron-catalyzed *ipso*-nitration of aryl halides via direct photoexcitation of iron(II) nitrate complexes without requiring an extra photoredox catalyst. By irradiating a solution containing an aryl halide, KNO_2, a catalytic amount of $FeSO_4$, and a Phen ligand with UV light irradiation at 254 nm, various aromatic nitro compounds including three pharmaceutical molecules are produced in this simple process. The utilization of previous iron complexes as photoredox catalysts is generally hampered because of the short lifetime of the excited state. However, under the combined effect of the nitro group and Phen, the iron complex's excited-state lifetime was obviously prolonged in this work. Furthermore, mechanistic investigations into iron catalysis are relatively difficult due to multiple valence states of iron catalysts and the competition of different mechanisms. The merits of this approach are illustrated by the novel iron-catalyzed *ipso*-nitration and the elucidation of the SET mechanism under photoinduced conditions. Moreover, the electron transfer from KNO_2, which is a weak electron donor, could also proceed smoothly through the formation of a photoexcited complex of $FeSO_4/KNO_2$/Phen. This work represents the first example for the photoinduced iron-catalyzed Ullmann-type couplings.

ASSOCIATED CONTENT

Supporting Information

The Supporting Information is available free of charge at https://pubs.acs.org/doi/10.1021/acscatal.1c02272.

Scheme 8. Proposed Mechanism

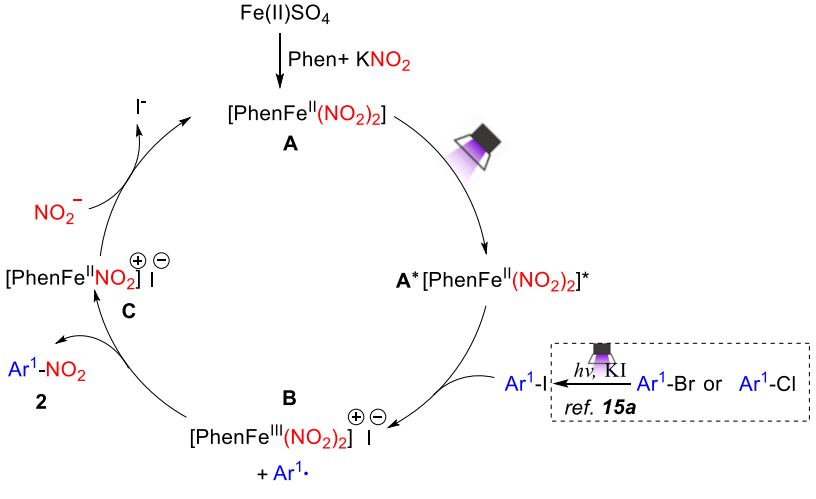

https://doi.org/10.1021/acscatal.1c02272
ACS Catal. 2021, 11, 9561−9568

General experimental procedures; characterization data; and copies of ^{1}H NMR and ^{13}C NMR spectra for the products (PDF)

X-ray data for compound **2q** (CIF)

AUTHOR INFORMATION

Corresponding Authors

Hao Xu − *Institute of Functional Organic Molecular Engineering, College of Chemistry and Chemical Engineering, Henan University, Kaifeng 475004, China; Key Laboratory of Bioorganic Phosphorus Chemistry and Chemical Biology (Ministry of Education), Department of Chemistry, Tsinghua University, Beijing 100084, China;* orcid.org/0000-0002-6069-3246; Email: xuhao@henu.edu.cn

Hai-Bei Li − *School of Ocean, Shandong University, Weihai 264209, China*; Email: lihaibei@sdu.edu.cn

Hua Fu − *Key Laboratory of Bioorganic Phosphorus Chemistry and Chemical Biology (Ministry of Education), Department of Chemistry, Tsinghua University, Beijing 100084, China;* orcid.org/0000-0001-7250-0053; Email: fuhua@mail.tsinghua.edu.cn

Authors

Cunluo Wu − *Institute of Functional Organic Molecular Engineering, College of Chemistry and Chemical Engineering, Henan University, Kaifeng 475004, China*

Qilong Bian − *Institute of Functional Organic Molecular Engineering, College of Chemistry and Chemical Engineering, Henan University, Kaifeng 475004, China*

Tao Ding − *Institute of Functional Organic Molecular Engineering, College of Chemistry and Chemical Engineering, Henan University, Kaifeng 475004, China; Key Laboratory of Bioorganic Phosphorus Chemistry and Chemical Biology (Ministry of Education), Department of Chemistry, Tsinghua University, Beijing 100084, China; School of Ocean, Shandong University, Weihai 264209, China*

Mingming Tang − *Institute of Functional Organic Molecular Engineering, College of Chemistry and Chemical Engineering, Henan University, Kaifeng 475004, China*

Wenkai Zhang − *Institute of Functional Organic Molecular Engineering, College of Chemistry and Chemical Engineering, Henan University, Kaifeng 475004, China;* orcid.org/0000-0003-3895-9033

Yuanqing Xu − *Institute of Functional Organic Molecular Engineering, College of Chemistry and Chemical Engineering, Henan University, Kaifeng 475004, China*

Baoying Liu − *Institute of Functional Organic Molecular Engineering, College of Chemistry and Chemical Engineering, Henan University, Kaifeng 475004, China*

Complete contact information is available at: https://pubs.acs.org/10.1021/acscatal.1c02272

Author Contributions

‖C.W. and Q.B. contributed equally to this work.

Notes

The authors declare no competing financial interest.

ACKNOWLEDGMENTS

This work was supported by the National Natural Science Foundation of China (Nos. U1904191, U1904184, U2004179, and 21403127), the Scientific Research Key Project Fund of Henan Provincial Education Department (No. 20A150002), the Science and Technology Develop Project of Kaifeng City (No. 1908011), the Fund of Young Scholars Program of Shandong University (No. YSPSDUWH). The authors thank the National Supercomputer Center in Tianjin-TianHe-1(A) for the computer time and the Super Computing Center, Shandong University, Weihai, for providing the supercomputing system.

REFERENCES

(1) (a) Belciug, M.-P.; Ananthanarayanan, V. S. Interaction of Calcium Channel Antagonists with Calcium: Structural Studies on Nicardipine and Its Ca^{2+} Complex. *J. Med. Chem.* **1994**, *37*, 4392−4399. (b) Parry, R.; Nishino, S.; Spain, J. Naturally-Occurring Nitro Compounds. *Nat. Prod. Rep.* **2011**, *28*, 152−167. (c) Fan, F.; Yao, Y.; Cai, L.; Cheng, L.; Tour, J. M.; Bard, A. J. Structure-Dependent Charge Transport and Storage in Self-Assembled Monolayers of Compounds of Interest in Molecular Electronics: Effects of Tip Material, Headgroup, and Surface Concentration. *J. Am. Chem. Soc.* **2004**, *126*, 4035−4042. (d) Mandalapu, D.; Kushwaha, B.; Gupta, S.; Singh, N.; Shukla, M.; Kumar, J.; Tanpula, D. K.; Sankhwar, S. N.; Maikhuri, J. P.; Siddiqi, M. I.; Lal, J.; Gupta, G.; Sharma, V. L. 2-Methyl-4/5-Nitroimidazole Derivatives Potentiated Against Sexually Transmitted Trichomonas: Design, synthesis, Biology and 3D-QSAR Study. *Eur. J. Med. Chem.* **2016**, *124*, 820−839. (e) Cheung, C. W.; Ma, J.; Hu, X. Manganese-Mediated Reductive Transamidation of Tertiary Amides with Nitroarenes. *J. Am. Chem. Soc.* **2018**, *140*, 6789−6792.

(2) (a) Ono, N. *The Nitro Group in Organic Synthesis*; Wiley-VCH: New York, 2001. (b) Olah, G. A.; Malhotra, R.; Narang, S. C. *Nitration: Methods and Mechanisms*; VCH: Weinheim, 1989. (c) Bharadwaj, S. K.; Boruah, P. K.; Gogoi, P. K. Phosphoric Acid Modified Montmorillonite Clay: A New Heterogeneous Catalyst for Nitration of Arenes. *Catal. Commun.* **2014**, *57*, 124−128.

(3) (a) Saito, S.; Koizumi, Y. Copper-Catalyzed Coupling of Aryl Halides and Nitrite Salts: A Mild Ullmann-Type Synthesis of Aromatic Nitro Compounds. *Tetrahedron Lett.* **2005**, *46*, 4715−4717. (b) Amal Joseph, P. J.; Priyadarshini, S.; Kantam, M. L.; Maheswaran, H. Copper Catalyzed *ipso*-nitration of Iodoarenes, Bromoarenes and Heterocyclic Haloarenes under Ligand-Free Conditions. *Tetrahedron Lett.* **2012**, *53*, 1511−1513. (c) Paik, S.; Jung, M. G. Rapid Microwave-Assisted Copper-Catalyzed Nitration of Aromatic Halides with Nitrite Salts. *Bull. Korean Chem. Soc.* **2012**, *33*, 689−691.

(4) (a) Fors, B. P.; Buchwald, S. L. Pd-Catalyzed Conversion of Aryl Chlorides, Triflates, and Nonaflates to Nitroaromatics. *J. Am. Chem. Soc.* **2009**, *131*, 12898−12899. (b) Prakash, G. K. S.; Mathew, T. *ipso*-Nitration of Arenes. *Angew. Chem., Int. Ed.* **2010**, *49*, 1726−1728.

(5) (a) Rana, S.; Biswas, J. P.; Paul, S.; Paika, A.; Maiti, D. Organic Synthesis with the Most Abundant Transition Metal-Iron: from Rust to Multitasking Catalysts. *Chem. Soc. Rev.* **2021**, *50*, 243−472. (b) Yoshida, T.; Ilies, L.; Nakamura, E. Iron-Catalyzed Borylation of Aryl Chlorides in the Presence of Potassium *t*-Butoxide. *ACS Catal.* **2017**, *7*, 3199−3203. (c) Yan, W.; Wang, Q.; Chen, Y.; Petersen, J. L.; Shi, X. Iron-Catalyzed C-O Bond Activation for the Synthesis of Propargyl-1,2,3-triazoles and 1,1-Bis-triazoles. *Org. Lett.* **2010**, *12*, 3308−3311.

(6) (a) Crockett, M. P.; Wong, A. S.; Li, B.; Byers, J. A. Rational Design of an Iron-Based Catalyst for Suzuki-Miyaura Cross-Couplings Involving Heteroaromatic Boronic Esters and Tertiary Alkyl Electrophiles. *Angew. Chem., Int. Ed.* **2020**, *59*, 5392−5397. (b) Pang, H.; Wang, Y.; Gallou, F.; Lipshutz, B. H. Fe-Catalyzed Reductive Couplings of Terminal (Hetero)Aryl Alkenes and Alkyl Halides under Aqueous Micellar Conditions. *J. Am. Chem. Soc.* **2019**, *141*, 17117−17124. (c) King, E. R.; Hennessy, E. T.; Betley, T. A. Catalytic C-H Bond Amination from High-Spin Iron Imido Complexes. *J. Am. Chem. Soc.* **2011**, *133*, 4917−4923. (d) Vallée, F.; Mousseau, J. J.; Charette, A. B. Iron-Catalyzed Direct Arylation

through an Aryl Radical Transfer Pathway. *J. Am. Chem. Soc.* **2010**, *132*, 1514−1516.
(7) Fürstner, A. Iron Catalysis in Organic Synthesis: A Critical Assessment of What It Takes To Make This Base Metal a Multitasking Champion. *ACS Cent. Sci.* **2016**, *2*, 778−789.
(8) (a) Creutz, S. E.; Lotito, K. J.; Fu, G. C.; Peters, J. C. Photoinduced Ullmann C-N Coupling: Demonstrating the Viability of a Radical Pathway. *Science* **2012**, *338*, 647−651. (b) Lim, C.-H.; Kudisch, M.; Liu, B.; Miyake, G. M. C-N Cross-Coupling via Photoexcitation of Nickel-Amine Complexes. *J. Am. Chem. Soc.* **2018**, *140*, 7667−7673. (c) Ziegler, D. T.; Choi, J.; Muñoz-Molina, J. M.; Bissember, A. C.; Peters, J. C.; Fu, G. C. A Versatile Approach to Ullmann C-N Couplings at Room Temperature: New Families of Nucleophiles and Electrophiles for Photoinduced, Copper-Catalyzed Processes. *J. Am. Chem. Soc.* **2013**, *135*, 13107−13112. (d) Uyeda, C.; Tan, Y.; Fu, G. C.; Peters, J. C. A New Family of Nucleophiles for Photoinduced, Copper-Catalyzed Cross-Couplings via Single-Electron Transfer: Reactions of Thiols with Aryl Halides Under Mild Conditions (0 °C). *J. Am. Chem. Soc.* **2013**, *135*, 9548−9552. (e) Tan, Y.; Muñoz-Molina, J. M.; Fu, G. C.; Peters, J. C. Oxygen Nucleophiles As Reaction Partners in Photoinduced, Copper-Catalyzed Cross-Couplings: *O*-Arylations of Phenols at Room Temperature. *Chem. Sci.* **2014**, *5*, 2831−2835. (f) Paria, S.; Reiser, O. Copper in Photocatalysis. *ChemCatChem* **2014**, *6*, 2477−2483.
(9) (a) Wei, X.; Abdiaj, I.; Sambiagio, C.; Li, C.; Zysman-Colman, Z.; Alcázar, J.; Noël, T. Visible-Light-Promoted Iron-Catalyzed $C(sp^2)$-$C(sp^3)$ Kumada Cross-Coupling in Flow. *Angew. Chem., Int. Ed.* **2019**, *58*, 13030−13034. (b) Neumeier, M.; Chakraborty, U.; Schaarschmidt, D.; de la Pena O'Shea, V.; Perez-Ruiz, R.; Jacobi von Wangelin, A. Combined Photoredox and Iron Catalysis for the Cyclotrimerization of Alkynes. *Angew. Chem., Int. Ed.* **2020**, *59*, 13473−13478. (c) Ye, J.; Miao, M.; Huang, H.; Yan, S.; Yin, Z.; Zhou, W.; Yu, D. Visible-Light-Driven Iron-Promoted Thiocarboxylation of Styrenes and Acrylates with CO_2. *Angew. Chem., Int. Ed.* **2017**, *56*, 15416−15420. (d) Huang, B.; Li, Y.; Yang, C.; Xia, W. Three-Component Aminoselenation of Alkenes via Visible-Light Enabled Fe-Catalysis. *Green Chem.* **2020**, *22*, 2804−2809. (e) Du, Y.; Zhou, C.; To, W. P.; Wang, H.; Che, C. Iron Porphyrin Catalysed Light Driven C-H Bond Amination and Alkene Aziridination with Organic Azides. *Chem. Sci.* **2020**, *11*, 4680−4686. (f) Woodhouse, M. D.; McCusker, J. K. Mechanistic Origin of Photoredox Catalysis Involving Iron(II) Polypyridyl Chromophores. *J. Am. Chem. Soc.* **2020**, *142*, 16229−16233. (g) Gualandi, A.; Marchini, M.; Mengozzi, L.; Natali, M.; Lucarini, M.; Ceroni, P.; Cozzi, P. G. Organocatalytic Enantioselective Alkylation of Aldehydes with $[Fe(bpy)_3]Br_2$ Catalyst and Visible Light. *ACS Catal.* **2015**, *5*, 5927−5931.
(10) Guo, Y.; Yang, J.; NuLi, Y.; Wang, J. Study of Electronic Effect of Grignard Reagents on Their Electrochemical Behavior. *Electrochem. Commun.* **2010**, *12*, 1671−1673.
(11) (a) Chábera, P.; Liu, Y.; Prakash, O.; Thyrhaug, E. N.; Honarfar, A. H.; Essén, S.; Fredin, L. A.; Harlang, T. C. B.; Kjær, K. S.; Handrup, K.; Ericson, F.; Tatsuno, H.; Morgan, K.; Schnadt, J.; Häggström, L.; Ericsson, T.; Sobkowiak, A.; Lidin, S.; Huang, P.; Styring, S.; Uhlig, J.; Bendix, J.; Lomoth, R.; Sundström, V.; Persson, P.; Wärnmark, K.; et al. A Low-Spin Fe(III) Complex with 100-ps Ligand-to-Metal Charge Transfer Photoluminescence. *Nature* **2017**, *543*, 695−699. (b) Büldt, L. A.; Guo, X.; Vogel, R.; Prescimone, A.; Wenger, O. S. A Tris(diisocyanide)chromium(0) Complex Is a Luminescent Analog of Fe(2,2′-Bipyridine)$_3^{2+}$. *J. Am. Chem. Soc.* **2017**, *139*, 985−992.
(12) Enneiymy, M.; Fioux, P.; Drian, C. L.; Ghimbeu, C. M.; Becht, J. M. Palladium Nanoparticles Embedded in Mesoporous Carbons As Efficient, Green and Reusable Catalysts for Mild Hydrgenations of Nitroarenes. *RSC Adv.* **2020**, *10*, 36741−36750.
(13) (a) Bistri, O.; Correa, A.; Bolm, C. Iron-Catalyzed C-O Cross-Couplings of Phenols with Aryl Iodides. *Angew. Chem., Int. Ed.* **2008**, *47*, 586−588. (b) Wu, W.; Wang, J.; Tsai, F. Y. A Reusable $FeCl_3$•$6H_2O$/Cationic 2,2′-Bipyridyl Catalytic System for the Coupling of Aryl Iodides with Thiols in Water under Aerobic Conditions. *Green Chem.* **2009**, *11*, 326−329. (c) Correa, A.; Bolm, C. Iron-Catalyzed *N*-Arylation of Nitrogen Nucleophiles. *Angew. Chem., Int. Ed.* **2007**, *46*, 8862−8865.
(14) Pause, L.; Robert, M.; Savéant, J. M. Can Single-Electron Transfer Break an Aromatic Carbon-Heteroatom Bond in One Step? A Novel Example of Transition between Stepwise and Concerted Mechanisms in the Reduction of Aromatic Iodides. *J. Am. Chem. Soc.* **1999**, *121*, 7158−7159.
(15) (a) Li, L.; Liu, W.; Zeng, H.; Mu, X.; Cosa, G.; Mi, Z.; Li, C. Photo-induced Metal-Catalyst-Free Aromatic Finkelstein Reaction. *J. Am. Chem. Soc.* **2015**, *137*, 8328−8331. (b) Liu, W.; Li, J.; Huang, C.; Li, C. Aromatic Chemistry in the Excited State: Facilitating Metal-Free Substitutions and Cross-Couplings. *Angew. Chem., Int. Ed.* **2020**, *59*, 1786−1796. (c) Qiu, G.; Li, Y.; Wu, J. Recent Developments for the Photoinduced Ar-X Bond Dissociation Reaction. *Org. Chem. Front.* **2016**, *3*, 1011−1027. (d) Jiang, M.; Li, H.; Yang, H.; Fu, H. Room-Temperature Arylation of Thiols: Breakthrough with Aryl Chlorides. *Angew. Chem., Int. Ed.* **2017**, *56*, 874−879. (e) Yang, X.; Liu, W.; Li, L.; Wei, W.; Li, C. Photo-induced Carboiodination: A Simple Way to Synthesize Functionalized Dihydrobenzofuransand Indolines. *Chem. - Eur. J.* **2016**, *22*, 15252−15256. (f) Peng, H.; Cai, R.; Xu, C.; Chen, H.; Shi, X. Nucleophile Promoted Gold Redox Catalysis with Diazonium Salts: C-Br, C-S and C-P Bond Formation through Catalytic Sandmeyer Coupling. *Chem. Sci.* **2016**, *7*, 6190−6196. (g) Motornov, V. A.; Muzalevskiy, V. M.; Tabolin, A. A.; Novikov, R. A.; Nelyubina, Y. V.; Nenajdenko, V. G.; Ioffe, S. L. Radical Nitration-Debromination of α-Bromo-α-fluoroalkenes as a Stereoselective Route to Aromatic α-Fluoronitroalkenes Functionalized Fluorinated Building Blocks for Organic Synthesis. *J. Org. Chem.* **2017**, *82*, 5274−5284.

https://doi.org/10.1021/acscatal.1c02272
ACS Catal. 2021, 11, 9561−9568